Super-virtual Interferometric Separation and Enhancement of Back-scattered Surface Waves

Bowen Guo, Sherif Hanafy and Gerard Schuster, King Abdullah University of Science and Technology*

SUMMARY

Back-scattered surface waves can be migrated to detect near-surface reflectors with steep dips. A robust surface-wave migration requires the prior separation of the back-scattered surface-wave events from the data. This separation is often difficult to implement because the back-scattered surface waves are masked by the incident surface waves. We mitigate this problem by using a super-virtual interferometric method to enhance and separate the back-scattered surface waves. The key idea is to calculate the virtual back-scattered surface waves by stacking the resulting virtual correlated and convolved traces associated with the incident and back-scattered waves. Stacking the virtual back-scattered surface waves improves their signal-to-noise ratio and separates the back-scattered surface-waves from the incident field. Both synthetic and field data results validate the robustness of this method.

INTRODUCTION

The collision of propagating surface waves with a near-surface fault generates back-scattered surface-waves (BSWs), which can be migrated to detect near-surface faults (Yu et al., 2014). A robust migration of BSWs requires the prior separation of the BSWs from the incident field. Such a separation is often difficult to implement because the BSWs are usually buried in other events. We mitigate this problem by using super-virtual interferometry to enhance and separate the BSW. The key idea is to create virtual CSGs dominated by BSWs by either cross-correlating or convolving the incident surface waves with the existing BSWs. Stacking the resulting super-virtual BSWs over different receivers improves their signal-to-noise ratio (SNR), and separates the BSWs from other events in the data.

The next section presents the theory for the super-virtual interferometric separation of the back-scattered events from the incident surface waves. This theory is based on the reciprocity equations of correlation and convolution types and super-virtual interferometry (Bharadwaj et al., 2011). The next section shows the numerical results with both synthetic data and field data. The synthetic data are generated for a 2D elastic model and the field data are for a seismic survey over a desert region with faults at the near surface. The final section presents conclusions.

THEORY

We assume surface waves $G(\mathbf{g}|\mathbf{s})$ contain incident surface waves $G(\mathbf{g}|\mathbf{s})^{inc}$ and back-scattered surface waves $G(\mathbf{g}|\mathbf{s})^{back}$:

$$G(\mathbf{g}|\mathbf{s}) = G(\mathbf{g}|\mathbf{s})^{inc} + G(\mathbf{g}|\mathbf{s})^{back}, \quad (1)$$

where $G(\mathbf{g}|\mathbf{s})$ represents the Green's function which is the vertical-component particle velocity of a surface wave with the virtical-component source at $\mathbf{s}$ and the receiver at $\mathbf{g}$.

Sources are placed at $\mathbf{s}$ and $\mathbf{s}'$, and one receiver is located at $\mathbf{g}$ on a land-recording line (Figure 1a). The recording line is divided into three segments l_1, l_2 and l_3 based on the positions of $\mathbf{s}$ and $\mathbf{s}'$. The fault is assumed to be at the right of $\mathbf{s}'$. The surface waves ignited by the source at $\mathbf{s}$ impinge on the fault, BSWs are generated and recorded at $\mathbf{g}$.

For the case of the receiver on l_1 as shown in Figure 1b, the cross-correlation between the BSWs $G(\mathbf{g}|\mathbf{s})^{back}$ and the inci-

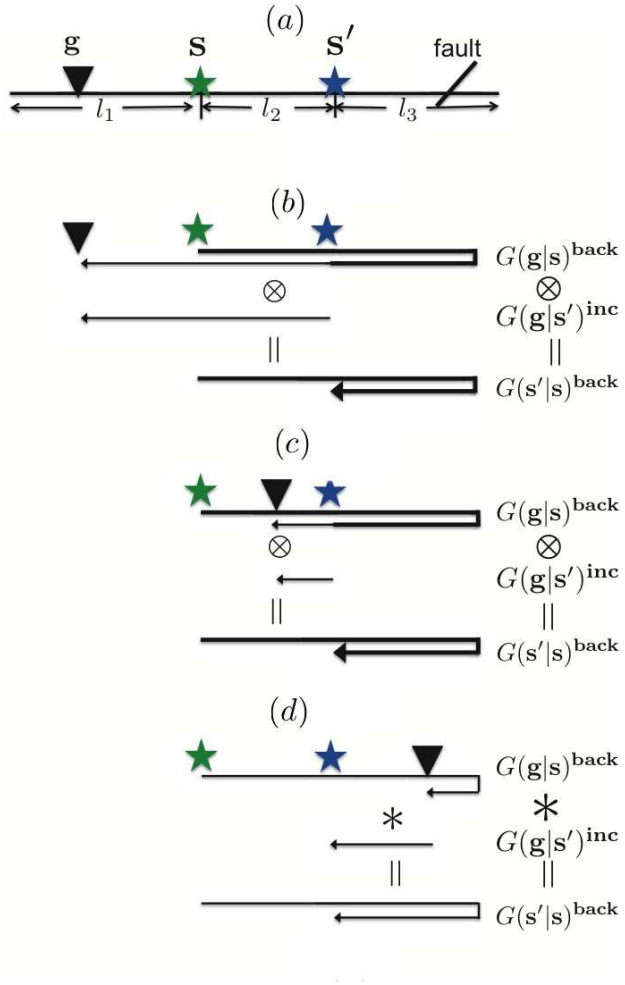

Figure 1: Workflow for the calculations of the virtual back-scattered surface waves. a) Data acquisition geometry, the cases for receivers along b) l_1, c) l_2 and d) l_3. In panels b and c, thicker arrows/lines represent the un-canceled raypaths, whose arrivals are amplified by the stacking over different receiver locations.

DOI http://dx.doi.org/10.1190/segam2015-5859452.1

dent surface waves $G(\mathbf{g}|\mathbf{s}')^{inc}$ cancels the phase of their common raypath (Schuster, 2009) and gives the virtual BSWs from $\mathbf{s}$ to $\mathbf{s}'$. The same virtual BSWs are given by all the receivers in l_1, thus stacking will improve their SNR. This procedure is summarized as

$$Im[\overline{G(\mathbf{s}'|\mathbf{s})^{back}}] \approx 2k \sum_{\mathbf{g}\in l_1} G(\mathbf{g}|\mathbf{s})^{back} \bigotimes G(\mathbf{g}|\mathbf{s}')^{inc}, \qquad (2)$$

where $\bigotimes$ represents cross-correlation, k represents the wavenumber of the surface wave, the $\overline{G(\mathbf{s}'|\mathbf{s})^{back}}$ represents the stacked virtual trace. Equation 2 is approximately valid because the cross-correlation only cancels the phase of the common raypath, but does not consider the dispersion of the surface waves. In practice, a deconvolution can be applied to the virtual BSWs to remove the dispersion in the surface waves.

For the case of the receiver on l_2 in Figure 1c, the same procedure as the previous case is repeated to calculate and stack the virtual BSWs:

$$Im[\overline{G(\mathbf{s}'|\mathbf{s})^{back}}] \approx 2k \sum_{\mathbf{g}\in l_2} G(\mathbf{g}|\mathbf{s})^{back} \bigotimes G(\mathbf{g}|\mathbf{s}')^{inc}. \qquad (3)$$

However, as shown in Figure 2, when the fault is located between the two source positions $\mathbf{s}$ and $\mathbf{s}'$, unphysical events are generated and enhanced by the cross-correlation and stacking in equations 2 and 3. These unphysical artifacts can be muted because they arrive earlier than the incident surface waves.

For the case of the receiver in l_3 as shown in Figure 1d, instead of cross-correlation, a convolution between the existing BSWs $G(\mathbf{g}|\mathbf{s})^{back}$ and the incident surface waves $G(\mathbf{g}|\mathbf{s}')^{inc}$

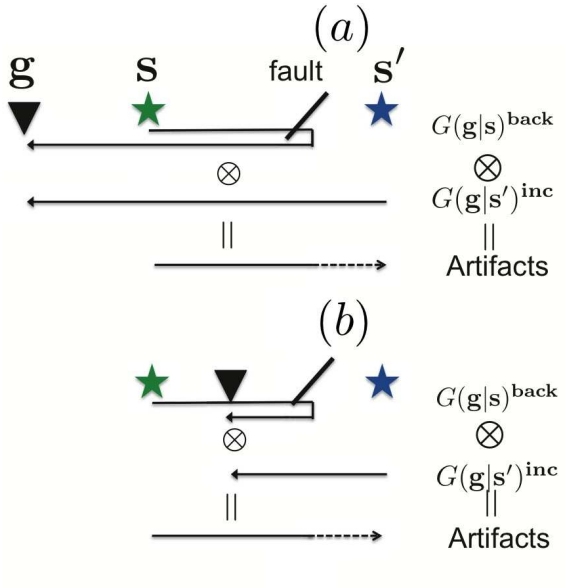

Figure 2: Illustration of the unphysical artifacts produced by the cross-correlations in equations 2 and 3. The dashed arrows represent the acausal raypaths.

elongates their virtual raypath (Schuster, 2009) and gives the virtual BSWs $G(\mathbf{s}'|\mathbf{s})^{back}$. As in the previous two cases, the virtual BSWs can be enhanced by the summation over all the receivers in l_3. This procedure is embodied in the equation

$$Im[\overline{G(\mathbf{s}'|\mathbf{s})^{back}}] \approx 2k \sum_{\mathbf{g}\in l_3} G(\mathbf{g}|\mathbf{s})^{back} * G(\mathbf{g}|\mathbf{s}')^{inc}. \qquad (4)$$

where $*$ represents convolution. Equation 4 will not produce the unphysical artifacts shown in Figure 2.

Theoretically, equations 2-4 give the same virtual BSWs, and so stacking of the output virtual BSWs of equations 2-4 enhances the resulting SNR even more. The concatenation of correlation, stacking and convolution, and stacking is identical to that given for super-virtual interferometry (Bharadwaj et al., 2011) except now back-scattered surface waves are reinforced. The above procedure is a special case of super-virtual interferometry (Bharadwaj et al., 2011), where the output traces are referred to as super-virtual traces.

The work flow is described as follows.

1. Mute the body waves,
2. Retain the incident surface waves and mute any other events,
3. Retain the BSWs and mute any other events,
4. Cross-correlate or convolve the incident surface waves with the existing BSWs and then stack the resulting virtual BSWs (equations 2-4).

In practice, steps 2 and 3 are optional, depending on the amplitudes of the incident and back-scattered surface waves. In most cases, strong incident surface waves are observed, and then step 2 can be skipped. If strong BSWs are observed, then step 3 can be skipped. Additionally, if steps 2 and 3 are implemented, the muting in these two steps does not need to be precise, but only requires an approximate removal of other events.

NUMERICAL RESULTS

Synthetic data (Figure 3b) are simulated by a 2D staggered-grid finite-difference elastic method (Virieux, 1986) based on the shear-wave velocity model V_s in Figure 3a. P-wave velocity is $\sqrt{3}V_s$. A fault is located in the velocity model so that BSWs are observed in the data. Random noise with the same strength as the BSWs is added to the data (Figure 3c). Incident surface waves are muted in Figure 3d, so that the traces in Figures 3c and 3d are used as the input $G(\mathbf{g}|\mathbf{s})^{back}$ and $G(\mathbf{g}|\mathbf{s}')^{inc}$ in equations 2-4, respectively. Based on equations 2-4, the virtual back-scatterd surface waves are calculated by cross-correlation (Figure 3e), convolution and stacking (Figure 3f). The unphysical artifacts discussed in Figure 2 are observed in Figure 3e. The shot gather comparison between Figures c-f and the trace comparison in Figure g reveal the SNR improvement of the BSWs, which validates equations 2-4.

For the field data, a total of 120 shot gathers were recorded near the Gulf of Aqaba in Saudi Arabia, where each shot gather

DOI http://dx.doi.org/10.1190/segam2015-5859452.1

contained 120 traces and the source and the receiver sampling intervals are both 2.4 m. The body waves in each common shot gather (CSG) are muted (Figures 5a and 5b). The traces in Figures 4b and 4c are used as approximations to $G(\mathbf{g}|\mathbf{s})^{back}$ and $G(\mathbf{g}|\mathbf{s}')^{inc}$, respectively. The convolution between $G(\mathbf{g}|\mathbf{s})^{back}$ and $G(\mathbf{g}|\mathbf{s}')^{inc}$ and stacking over different $\mathbf{g}$ positions generate the traces that mostly contain the virtual BSWs seen in Figure 4d. This result shows that even when the input $G(\mathbf{g}|\mathbf{s})^{back}$ contain many events which are not the existing BSWs, the reconstructed virtual BSWs are still distict. This phenomenon shows the robustness of this method. Same results are also observed in other shot gathers as shown in Figures 4e-4h. All the reconstructed virtual BSWs indicate a fault position around $X = 150$ m. The same fault position is suggested by the traveltime and the resistivity tomograms (Figure 4i).

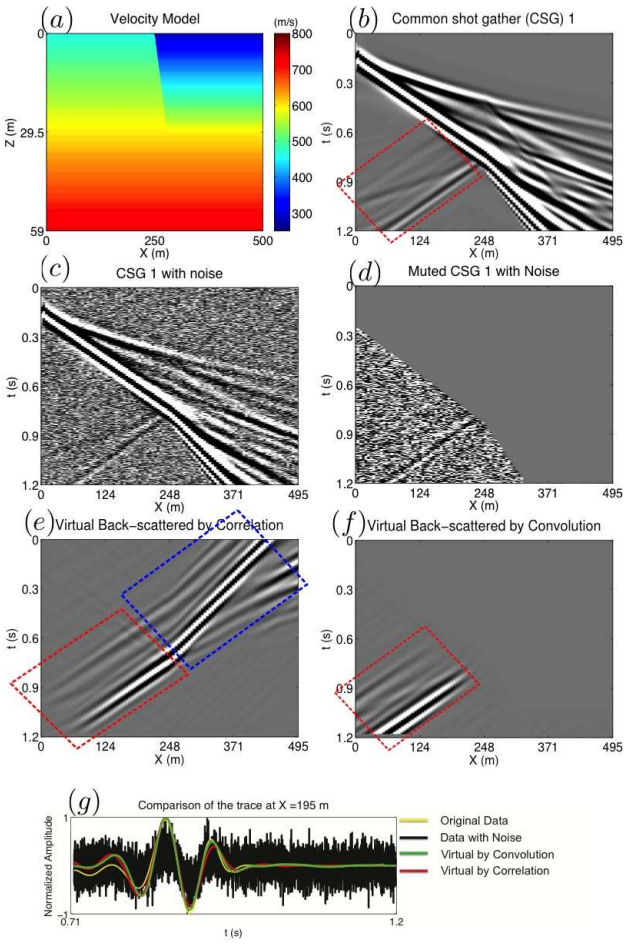

Figure 3: Synthetic data results. Red dashed squares suggest BSWs. a) Shear wave velocity model, b) 1^{st} common shot gather (CSG 1), c) CSG 1 with the random noise added, d) c) Noised CSG 1 the incident surface waves muted, e) Virtual BSWs by cross-correlation and stacking. Blue dashed square suggests the cross-correlation artifacts. f) Virtual BSWs by convolution and stacking, g) Comparison of the trace at $X = 195$ m.

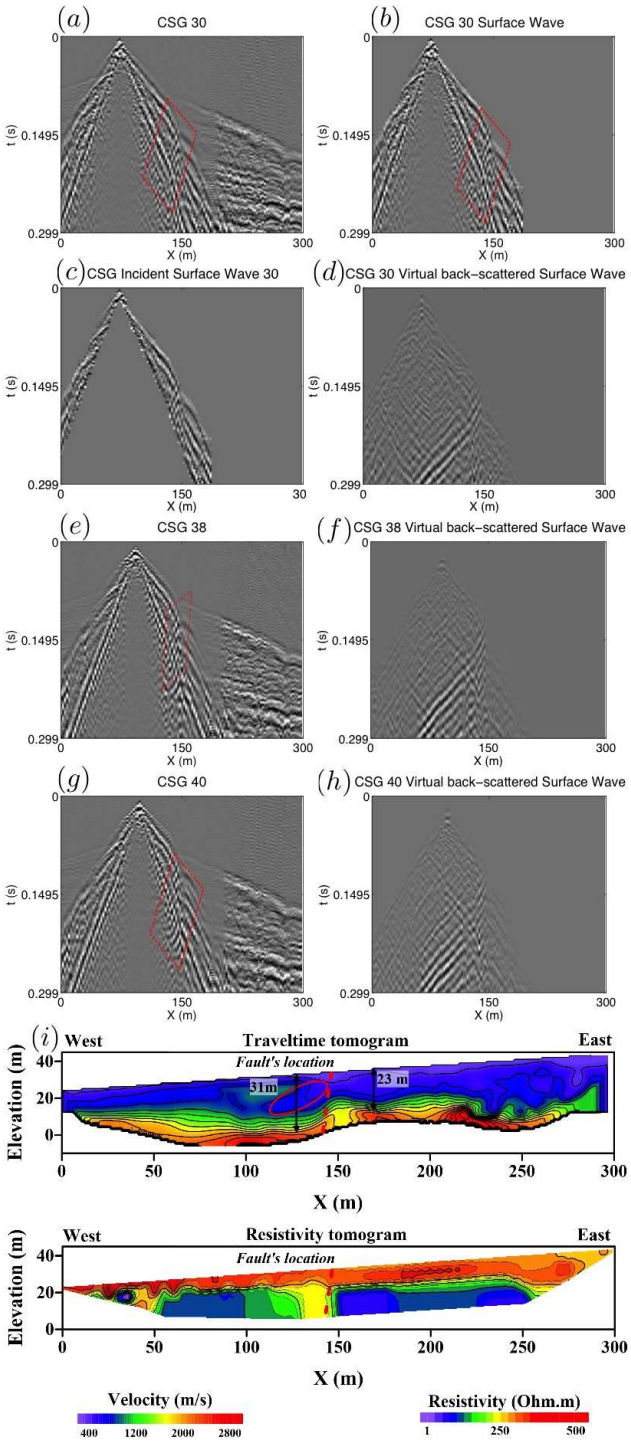

Figure 4: Field data results. Red dashed squares suggest BSWs. a) 30^{th} common shot gather (CSG 30), b) CSG 30 after muting body waves, c) Retaining incident surface waves and muting other events, d) Reconstructed virtual BSWs, e) CSG 38, f) Virtual BSWs of CSG 38, g) CSG 40, h) Virtual BSWs of CSG 40, i) Traveltime and resistivity tomogram results.

DOI http://dx.doi.org/10.1190/segam2015-5859452.1

CONCLUSIONS

We show that the back-scattered surface waves can be enhanced and separated by a super-virtual interferometric method, which stacks the correlated and convolved traces associated with the incident surface waves and the existing back-scattered surface waves. This method is robust, easy to implement and not reliant on the velocity information. Both synthetic and field data results show the enhancement of the separation of the BSWs from other events. Our future research direction is to extend this method to a 3D exploration data for land environments.

ACKNOWLEDGMENTS

We would like to thank the 2014 sponsors of the CSIM Consortium (http://csim.kaust.edu.sa/web/) for their fi- nancial support. The computation resource provided by the high performance computing (HPC) center of King Abdullah University of Science and Technology (KAUST) is greatly appreciated. We also thank anonymous CSIM members for their efforts in the development of this work.

DOI http://dx.doi.org/10.1190/segam2015-5859452.1

EDITED REFERENCES

Note: This reference list is a copyedited version of the reference list submitted by the author. Reference lists for the 2015 SEG Technical Program Expanded Abstracts have been copyedited so that references provided with the online metadata for each paper will achieve a high degree of linking to cited sources that appear on the Web.

REFERENCES

Bharadwaj, P., G. T. Schuster, I. Mallinson, 2011, Supervirtual refraction interferometry: Theory: 81st Annual International Meeting, SEG, Expanded Abstracts, **30**, 3809.

Schuster, G., 2009, Seismic interferometry: Cambridge University Press. http://dx.doi.org/10.1017/CBO9780511581557.

Virieux, J., 1986, P-SV wave propagation in heterogeneous media: Velocity-stress finite-difference method: Geophysics, **51**, 889–901. http://dx.doi.org/10.1190/1.1442147.

Yu, H., B. Guo, S. Hanafy, F.-C. Lin, and G. T. Schuster, 2014, Direct detection of near-surface faults by migration of backscattered surface waves: 84th Annual International Meeting, SEG, Expanded Abstracts, 2135–2139.